Ceramics International 50 (2024) 26059–26064

Contents lists available at ScienceDirect

Ceramics International

journal homepage: www.elsevier.com/locate/ceramint

Efficient single-step mechanosynthesis route of nanostructured $Hf_{0.2}Nb_{0.2}Ta_{0.2}V_{0.2}Zr_{0.2}C_{0.5}N_{0.5}$ High Entropy Carbonitride Powder

E. Chicardi [a,*], S. Gallego-Parra [b], C. Salvo [c], R. Sepúlveda [a]

[a] Departamento de Ingeniería y Ciencia de los Materiales y del Transporte, Escuela Técnica Superior de Ingeniería, Universidad de Sevilla, Spain
[b] European Synchrotron Radiation Facility, 71 Avenue des Martyrs, 38000 Grenoble, France
[c] Departamento de Ingeniería Mecánica, Facultad de Ingeniería, Universidad del Bío-Bío, Concepción, Chile

ARTICLE INFO

Keywords:
Mechanosynthesis
Carbonitride
High entropy ceramic
Powder metallurgy
Solid solution

ABSTRACT

Nowadays high entropy carbides (HECs) are an important group of advanced ceramics. They are composed by at least by five transition metals (TMs) in nearly equiatomic proportion and disordered distributed in the cationic sublattice of face centered cubic structures, with carbon atoms in the octahedral interstitial voids, with general formula (TM1,TM2,TM3,TM4,TM5)C. These HECs belong to the recent novel group of ultra-high temperature ceramics (UHTCs), with superior properties in comparison with the constituent binary carbides. However, the synthesis of those HECs can be modified to develop high entropy carbonitrides, HECNs, where the C are partially substituted by N, to form a solid solution in the anionic sublattice, with expected improved properties as UHTCs, but they are in an incipient state of development. Here, we report the synthesis and deep characterization of a non-previously obtained $Hf_{0.2}Nb_{0.2}Ta_{0.2}V_{0.2}Zr_{0.2}C_{0.5}N_{0.5}$ HECN, via a facile, single step and reproducible solid-gas reaction mechanosynthesis route. The synthesis was successfully completed in a planetary ball mill device, after 2h of milling time, at 400 rpm and using a ball-to- powder ratio of 60:1 in a pure N_2 atmosphere at room temperature. The as-synthesized HECNs powdered showed nanostructured morphology and outstanding high-temperature oxidation resistance up to 1500 °C.

1. Introduction

High entropy materials (HEMs) were firstly reported for high entropy alloys (HEAs) in 2004 by Yeh et al. [1], they are a novel group of advanced materials formed by five or more main elements in equal or near equal atomic proportion [2]. This high number of elements randomly distributed in the crystalline structure causes an entropic stabilization of the solid solutions, mainly face centered cubic (fcc) structures, against the formation of ordered compounds. Due to this compositional aspect, the properties of HEMs are in general superior when compared to similar traditional materials [3].

Nowadays, the high entropy effect is accepted to be extended to ceramics, forming as a general concept the synthesis of novel high entropy ceramics (HEKs, to differentiate to the high entropy carbides, HECs). In this context, in the last years, it stands out the growing interest of the research community for the called HECs [4–6], formed by five transition metals (TMs). More especially those of the IVB (Ti,Zr,Hf), VB (V,Nb,Ta) and VIB (Cr,Mo,W) groups, being disorderedly distributed in the cationic sublattice of fcc structures, and carbon in the octahedral interstitial voids, with general formula (TM1,TM2,TM3,TM4,TM5)C. These HECs belong to the recent novel group of ultra-high temperature ceramics (UHTCs), with superior properties in comparison with the most common binary carbides, such as higher melting temperature, hardness, and mechanical strength, as well as more thermochemical stability, better extreme heat, excellent oxidation and wear resistances, adjustable thermal conductivity, higher radiation resistance to neutrons and higher biocompatibility [5]. All these outstanding improved properties make them a promissory advanced ceramics group for potential applications in diverse industries, such as aerospace (hypersonic light, rocket propulsion), solar energy as thermal isolated material for concentrating solar power plants and nuclear fusion reactor as thermal and irradiation insulation, as plasma facing materials (PFM), among others [7]. All those applications have in common the harsh environment and extreme conditions that must stand the HECs [8].

Going even further, the possibility to generate a solid solution in the anionic sublattice in the HECs instead, evolves the synthesis of high entropy carbonitrides (HECNs). In this case, some atoms of C are replaced to N in the same crystalline position, analogous to the synthesis

* Corresponding author.
E-mail address: echicardi@us.es (E. Chicardi).

https://doi.org/10.1016/j.ceramint.2024.04.347
Received 29 March 2024; Received in revised form 23 April 2024; Accepted 25 April 2024
Available online 26 April 2024

of single of complex metal carbonitrides, such as Ti(C,N), (Ti,Ta)(C,N), (Ti,Nb,Ta)(C,N), (Hf,Zr)(C,N), etc [9–13]. In this sense, it is widely reported the improvement of the properties of carbonitrides in comparison with carbides or nitrides, such as better oxidation resistance, etc.

Furthermore, the extension of HECs to HECNs has been already published in a scarce works. Che et al. [14]. have developed (Cr,Zr,Nb,Hf,Ta)(C,N), (Cr,Zr,Nb,Hf,Ta,Ti)(C,N), and (Cr,Zr,Nb,Hf,Ta,Ti, V)(C,N) by mixture of different single nitride and carbides using reactive sintering of a compacted mixture at really high temperature, up to 2215 °C. Jiang et al. [15]. synthesized a (CuNiTiNbCr)C_xN_y film by a complex high energy double-target co-sputtering method using high purity of metals and graphite targets. Another thin film sputtering method, a double glow plasma alloy was selected by Yin et al. [16] to develop a coating of (Cr,Hf,Nb,Ta,Ti)(C,N) HECN. However, the most widely extended method to prepare HECNs is based on the use of the different single metallic oxides as precursors and graphite or carbon black, and subsequent reactive sintering in a reductant flow of pure nitrogen (N_2) at high pressure (400–600 MPa) and temperatures, up to 2100 °C. In this sense, Ma S. et al. [17], Jing et al. [18], Li et al. [19], and Ma J. et al. [20] have obtained (HfZrTaNbTi)(C,N), (Ti,V,Nb,Ta,Mo)(C,N), (Ti,Ta,Nb,Zr,W)(C,N), and (Ti,Zr,V,Nb,Ta)(C,N) HECNs, respectively. All of them were synthesized employing high energy synthesis routes, high temperature, pressure, voltage, and/or intensity. In addition, these routes were developed to manufacture thin film and/or bulk materials and only some compositions have been developed at this time.

The main goal of this work is to demonstrate a new synthesis route for a novel and non-developed $Hf_{0.2}Nb_{0.2}Ta_{0.2}V_{0.2}Zr_{0.2}C_{0.5}N_{0.5}$ HECN. This synthesis route is based on a facile, simple, reproducible, and low temperature mechanosynthesis solid-gas reaction method, starting from single powdered metals, charcoal, and nitrogen gas as atmosphere reactant. The obtained nanostructured powders could be later used as raw materials for coatings, ceramic matrix composites, or cermets.

2. Materials and method

2.1. Synthesis of the $Hf_{0.2}Nb_{0.2}Ta_{0.2}V_{0.2}Zr_{0.2}C_{0.5}N_{0.5}$ high entropy carbonitride

For the synthesis of the powdered and nanostructured HECN with nominal composition of $Hf_{0.2}Nb_{0.2}Ta_{0.2}V_{0.2}Zr_{0.2}C_{0.5}N_{0.5}$, powdered Hf (CAS number 7440-58-6, 325 mesh, 99.6 % of purity, Strem Chemical), Nb (CAS number 7440-03-1, 325 mesh, 99.8 of purity, Strem Chemical), Ta (CAS number 7440-25-7325 mesh, 99.98 of purity, Strem Chemical), V (CAS number 7440-62-2, 325 mesh, 99.5 of purity, Strem Chemical), Zr (CAS number 7440-67-7, 325 mesh, 99.5 of purity, Strem Chemical), extra pure activated charcoal as C source (CAS number 7440-44-0, 98 % of purity, Merck supplier), and N_2 gas (99.999 % of purity, Abelló Linde) as reagents. For clarity and ease of reading, henceforth we will refer to the as-synthesized HECN as (HfNbTaVZr)(CN). Thus, 1 g of the stoichiometric amount of the solid reagents (Hf, Nb, Ta, V, Zr, C) were placed in a 125 mL stainless steel vial with 9 stainless steel balls (diameter of 10 mm and 6.7 g per ball), corresponding to a high ball to powder ratio (BPR) of 60:1 for each milling process. In addition, the nitrogen gas was introduced in the vial up to a static pressure of 5 atm using a non-return valve. The powder mixtures were then ball milled in a PM100 planetary ball mill (Retsch) at 400 rpm of spinning rate during 0.5h, 2h and 20 h of milling time, and a rotation-to-revolution speed ratio of −2. After the milling process, the as-milled powders remained in the vial until reach room temperature to minimized possible oxidation of powders. Finally, they were carefully collected for further characterization.

2.2. Microstructural and thermal stability characterization

To determine the crystal structure evolution during mechanosynthesis, X-ray diffractograms were collected for the as-milled mixtures at different milling times between 0.5h and 20h, using a D8 Discover A25 (Bruker), with Bragg-Brentano geometry, in a 20°-80° of 2 theta degree, and step of 0.03° and time per step of 0.5 s·step^{-1}. The X'Pert HighScore Plus, from the Malvern Panalytical Company was used for the experimentally collected XRDs manipulation. In addition, the powder diffraction file PDF4+ inorganic database from the International Centre for Diffraction Data (ICDD) was used to elucidate the phase structure synthesized. The crystalline domain size (D) was estimated by the Scherrer equation, as follow (equation (1)):

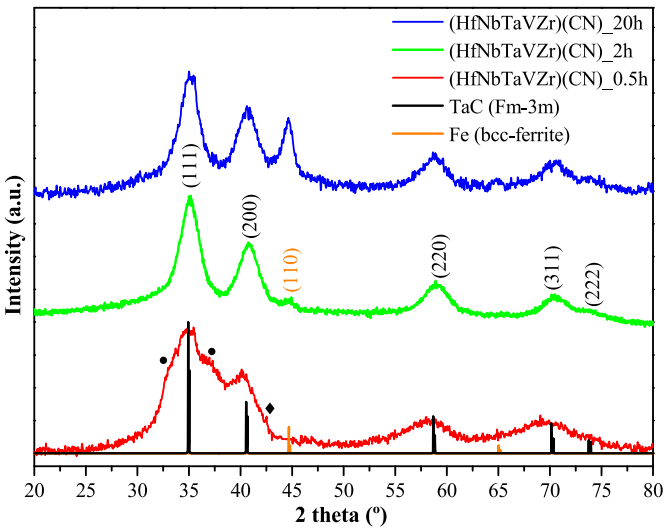

Fig. 1. X-Ray Diffractogram for the as synthesized $Hf_{0.2}Nb_{0.2}Ta_{0.2}V_{0.2}Zr_{0.2}C_{0.5}N_{0.5}$ high entropy carbonitride. (•) Unreacted Zr–Hf; (◆) Unreacted V.

$$D = \frac{K \cdot \lambda}{\beta \cdot \cos\theta} \quad (1)$$

where K is a shape factor of 0.89, attending to the cubic structure of HECN, λ is the X-ray wavelength used for XRD pattern (Cu, kα = 1.54 Å), and β the measured integral breath (defined as the net peak area/peak height ratio), and cos θ, the cosine of theta degree.

The degree of C and N incorporated to the powder during milling was determined by elemental analysis using a Leco instrument (model Truspec CHNS micro). Subsequently, to corroborate the microstructure, crystalline structure of phases, and the distribution of elements, the transmission electron microscopy study (TEM, HRTEM, selected area electron diffraction (SAED), high-angle annular dark-field (HAADF), and energy-dispersive X-ray spectroscopy (EDS) images) was carried out on a FEI Talos™ F200S scanning/transmission electron microscope at an acceleration voltage of 200 kV (point resolution = 0.25 nm). Samples for TEM were prepared by dropping sample dispersion in ethanol onto carbon-coated copper grids and letting the ethanol evaporate at room temperature and vacuum. The JEMS software was used to resolve the structures obtained by SAED.

Finally, a simultaneous differential scanning calorimetry-thermal gravimetric analysis (DSC-TGA) was conducted in a SDT Q600II (TA-Instrument) device, up to 1500 °C at 10 °C·min^{-1} in to determine the chemical stability of the as-synthesized HECN in static air. Approximately 100 mg of the as-synthesized HECN was used for each experiment.

3. Results and discussions

Fig. 1 displays the diffractograms obtained for the mixture of powders milled at 0.5, 2 and 20h. The diffractogram called as (HfNbTaVZr)(CN)_0.5h showed the presence of a NaCl-like fcc structure with the space group symmetry (SGS) *Fm-3m* (no. 225), analogous to the single

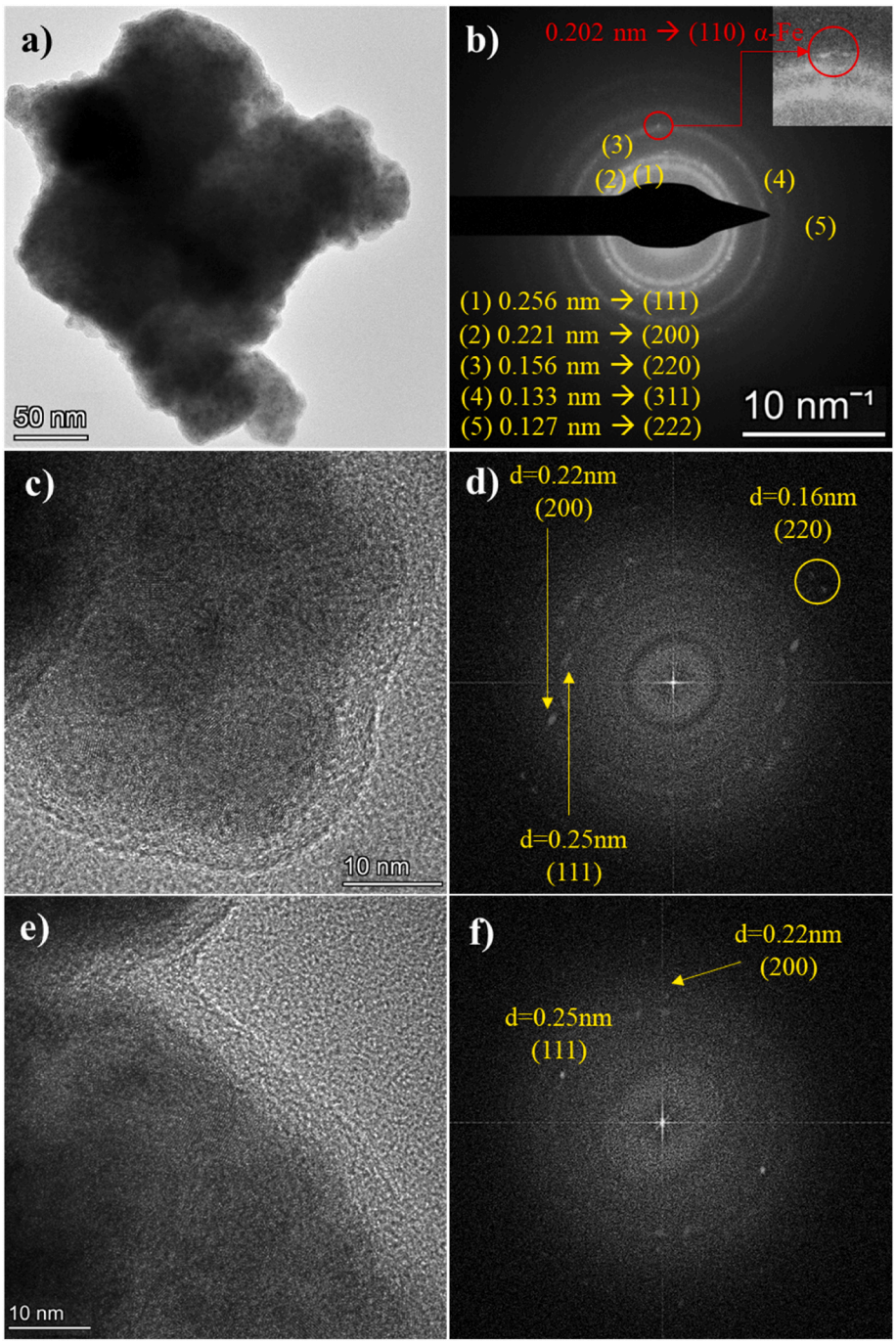

Fig. 2. Transmission electron microscopy images for the (HfNbTaVZr)(CN)_2h as-synthesized specimen a) Low resolution image; b) Electron diffraction pattern of the particle showed in a); c-f) High resolution images and the corresponding fast Fourier transform (FFT) images.

carbides and nitrides from the initial transition metals used. For comparison purposes, the XRD pattern of the TaC (ref. no 00-35-0810) has been included, corroborating the same crystalline structure. However, the presence of three resolved extra peaks indicates the incomplete formation of the single (HfNbTaVZr)(CN) HECN. The two most intense peaks can be assigned to a hexagonal close-packed phase. Attending to the crystalline structure of the metallic reagents, both can be assigned to Zr (hcp, P63/mmc of SGS, and ref. pattern no. 00-005-0665), and Hf (hcp, P63/mmc of SGS, and ref. pattern no. 00-038-1478). The third minor peak matches with unreacted V (bcc, Im3m of SGS and ref. pattern no. 00-022-1058). After 2h of milling time, the as-synthesized (HfNbTaVZr)(CN)_2h, clearly showed the presence of a single phase corresponding with the same fcc structure with SGS *Fm-3m*, phase match with the metal single carbides and nitrides of transition metals used extracted from the PDF4+-ICDD database (HfC (00-39-1491), NbC (00-36-1364), TaC (00-35-0810), VC (01-073-0476), ZrC (00-035-0784), HfN (00-033-0592), NbN (00-020-0801), TaN (039–1485), VN (035–0768), and ZrN (031–1493)). All of them exhibit the same SGS *Fm-3m* structure and is analogous to the HEC previously synthesized in Ar atmosphere [4].

With the lattice parameters of those single carbides and nitrides, the theoretical lattice for the as-synthesized (HfNbTaVZr)(CN) HECN can be determined as a = b = c = 4.440 Å, attending to the Vegard's law. By the measurement of the individually fitted peaks corresponding to the (111), (200), (222), (311) and (222) crystallographic planes, with interplanar distances (d) of 2.56 Å, 2.21 Å, 1.57 Å, 1.33 Å, and 1.28 Å

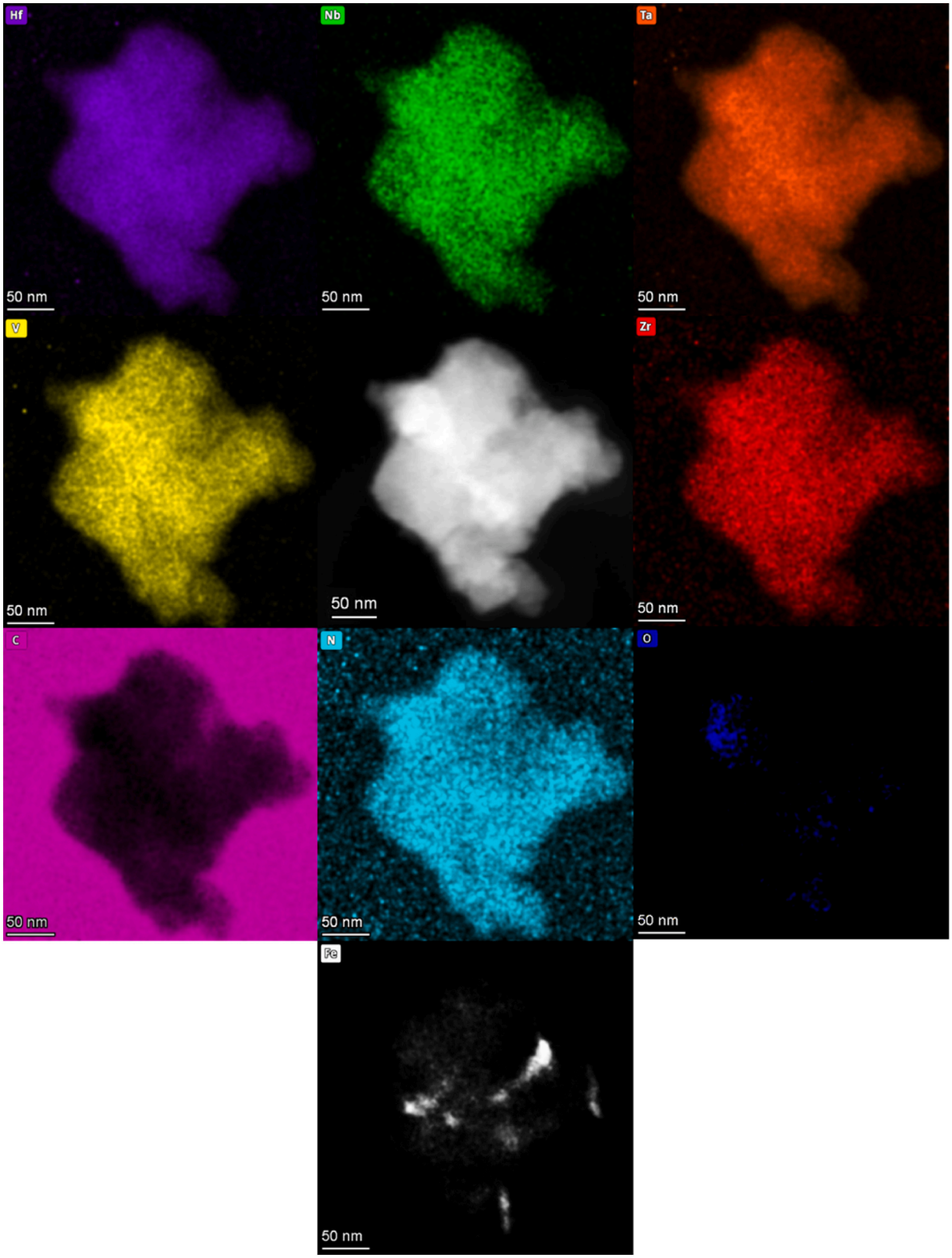

Fig. 3. EDS images in STEM mode showing the optimal distribution of elements for the (HfNbTaVZr)(CN)_2h. Purple = Hf; Green = Nb; Orange = Ta; Yellow = V; Grey = STEM-HAADF image; Red = N; Pink = c; Light blue = N; Blue = O; White = Fe. (For interpretation of the references to colour in this figure legend, the reader is referred to the Web version of this article.)

respectively, the experimental lattice parameter was also determined, using equation (2) for fcc structures, giving a value of 4.444 ± 0.004 Å. In a previous work, the obtained lattice parameter for the analogous carbide (HfNbTaVZr)C was a = b = c = 4.491 ± 0.023 Å [4], a higher lattice parameter value as compared to the respective carbonitride, following the same trend of all single nitrides showed lower lattice parameter than the analogous carbides. Then, both close values and the total absence of another phases, can corroborate the formation of the abovementioned carbonitride.

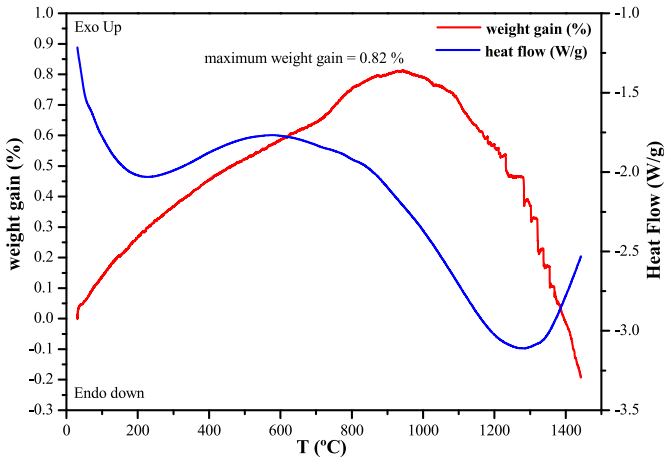

Fig. 4. Simultaneous DSC-TGA for the as-synthesized (HfNbTaVZr)(CN)_2h. Red line: Weight gain (%); Blue line: Heat Flow. (For interpretation of the references to colour in this figure legend, the reader is referred to the Web version of this article.)

$$a = b = c = d \cdot \sqrt{h^2 \cdot k^2 \cdot l^2} \quad (2)$$

The crystalline domain size (D) determined by the Scherrer formula for the (HfNbTaVZr)(CN)_2h gave a value of 3.8 ± 1.9 nm, showed the nanostructured characteristic of the as-synthesized powdered (HfNbTaVZr)(CN) HECN. The presence of nitrogen in the (HfNbTaVZr)(CN)_2h HECN was also corroborated by elemental analysis, giving an atomic ratio of C/N equal to 1.08, corresponding to a 52 at. % of C and 48 at. % of N, close to the anionic sublattice nominal composition designed.

Another slight peak was also indexed in the as-synthesized (HfNbTaVZr)(CN)_2h sample. This peak corresponds to the (110) crystallographic plane of ferrite (α-Fe, body centered cubic structure (bcc), ref. code no. 00-006-0969 in the DPF4+ database), coming from the vial and balls stainless steel milling media used. To ensure the complete synthesis and stability of the (HfNbTaVZr)(CN) HECN, the milling time was extended from 2 h up to 20 h in 2-h intervals. Since no differences were found in the transformation of powder milled in this period, except for the Fe contamination, only the powders milled for 20 h have been included in Fig. 1 to enhance the visual appeal of the corresponding graph.Thus, in the corresponding diffractogram (Fig. 1) it is possible to observe how the peaks for the HECN remained invariant, due to the successful formation of the HECN. However, the higher milling time applied together with the abrasive nature of the HECN ceramic synthesized produced the higher contamination of the specimens with Fe, suggesting then the 2h of milling time as optimal time to synthesize the expected (HfNbTaVZr)(CN) HECN.

In addition, a deep transmission electron microscopy (TEM) characterization was carried out to claim the formation and composition of the $Hf_{0.2}Nb_{0.2}Ta_{0.2}V_{0.2}Zr_{0.2}C_{0.5}N_{0.5}$ HECN, in the (HfNbTaVZr)(CN)_2h specimen, as can be seen observed in Fig. 2. Thus, the nanostructured character of the powder was also corroborated in Fig. 2a by the image of a representative single particle and in the electron diffraction (ED) image, Fig. 2b, by the presence of diffraction ring patterns, characteristics of a high numbers of particles randomly oriented. In turn, in the same ED image collected from a wide group of particles could be indexed the interplanar distances (d) corresponding to the (111), (200), (220) (311) and (222) crystallographic planes. The calculated "d" values determined were 0.256 nm, 0.221 nm, 0.156 nm, 0.133 nm, and 0.127 nm, respectively, in agreement with the values previously determined by XRD.

The HAADF-EDS analysis (Fig. 3) revealed the homogeneous spatial distribution of the five metallic elements corresponding to the cationic sublattice, i.e., Hf, Nb, Ta, V and Zr, and the nonmetallic elements, mainly nitrogen. The carbon distribution was not possible to determine due to the presence of the amorphous carbon in the TEM grid. Also, a small area of Fe and O could be detected, corresponding to the Fe contamination from milling media (average value determined of 1.1 wt % by scanning of different area) and probably some minor oxides due to the remaining slight amount of oxygen during mechanosynthesis process. The oxide cannot be assigned to a particular metal, suggesting the presence of a complex oxide.

Finally, a simultaneous DSC-TGA analysis was carried out up to 1500 °C (Fig. 4) to study the chemical stability of the as-synthesized HECN powder at high temperature. There is a practically negligible increase in weight gain of 0.82 wt% starting at 200 °C, reaching its maximum at 1000 °C. Above that temperature, almost the same weight gained of loose. The heat flow curve showed an exothermic peak near 550 °C, to later show a minimum endothermic peak about 1300 °C. Attending to the Baur-Glaessner diagram of Fe–O–C, the initial gained weight can be attributed to the sequential oxidation of Fe_3O_4 as: Fe → Fe_XO → Fe_3O_4 [21], starting at temperatures lower than 200 °C and reaching it maximum at 1000 °C. After that, the weight loss could be attributed to the reduction of Fe_3O_4 probably due to the presence of minor free unreacted carbon, with the subsequently formation of CO_2. This assertion is based in the non-stoichiometric nature of carbonitrides developed by mechanosynthesis [22]. Thus, the most important aspect is the high stability of the HECN, even up to 1500 °C. It is important to highlight that this study was carried out on the powdered HECN, with high specific surface and highly mechanical activated due to milling process.

4. Conclusions

A novel material, Hf0.2Nb0.2Ta0.2V0.2Zr0.2C0.5N0.5 HECN, has been synthesized for the first time via a mechanosynthesis route using a solid-gas reaction with elemental transition metals, activated carbon, and nitrogen gas as reagents. The synthesis process necessitated a high-energy ball milling procedure with a powder to ball ratio of 40:1, and an optimal milling time of 2 h.

The as-synthesized powdered HECN exhibited an ideal distribution of each element in both the cationic sublattice (Hf, Nb, Ta, V, and Zr) and the anionic sublattice (C and N), along with a nanostructure characteristic. Furthermore, a DSC-TGA study revealed high thermal and chemical stability up to 1500 °C. The obtained powdered HECN, in contrast to the typical bulk material observed in similar HECN synthesized through alternative routes, it is suitable for coatings and/or ceramic phases in cermets or ceramic matrix composites.

CRediT authorship contribution statement

E. Chicardi: Writing – review & editing, Writing – original draft, Visualization, Validation, Supervision, Software, Methodology, Investigation, Funding acquisition, Formal analysis, Data curation, Conceptualization. **S. Gallego-Parra:** Writing – review & editing, Writing – original draft, Software, Data curation. **C. Salvo:** Writing – review & editing, Methodology, Formal analysis, Data curation. **R. Sepúlveda:** Writing – review & editing, Supervision, Software, Methodology, Formal analysis, Data curation.

Declaration of competing interest

The authors declare that they have no known competing financial interests or personal relationships that could have appeared to influence the work reported in this paper.

References

[1] J.W. Yeh, S.K. Chen, S.J. Lin, J.Y. Gan, T.S. Chin, T.T. Shun, C.H. Tsau, S.Y. Chang, Nanostructured high-entropy alloys with multiple principal elements: novel alloy

design concepts and outcomes, Adv. Eng. Mater. 6 (2004) 299–303, https://doi.org/10.1002/adem.200300567.
[2] J. Normand, R. Moriche, C. García-Garrido, R.E. Sepúlveda Ferrer, E. Chicardi, Development of a tinbtamozr-based high entropy alloy with low young's modulus by mechanical alloying route, Metals 10 (2020) 1–15, https://doi.org/10.3390/met10111463.
[3] Y.F. Ye, Q. Wang, J. Lu, C.T. Liu, Y. Yang, High-entropy alloy: challenges and prospects, Mater. Today 19 (2016) 349–362, https://doi.org/10.1016/j.mattod.2015.11.026.
[4] E. Chicardi, C. García-Garrido, J. Hernández-Saz, F.J. Gotor, Synthesis of all equiatomic five-transition metals High Entropy Carbides of the IVB (Ti, Zr, Hf) and VB (V, Nb, Ta) groups by a low temperature route, Ceram. Int. 46 (2020) 21421–21430, https://doi.org/10.1016/j.ceramint.2020.05.240.
[5] M.A. Tunes, S. Fritze, B. Osinger, P. Willenshofer, A.M. Alvarado, E. Martinez, A. S. Menon, P. Ström, G. Greaves, E. Lewin, U. Jansson, S. Pogatscher, T.A. Saleh, V. M. Vishnyakov, O. El-Atwani, From high-entropy alloys to high-entropy ceramics: the radiation-resistant highly concentrated refractory carbide (CrNbTaTiW)C, Acta Mater. 250 (2023) 118856, https://doi.org/10.1016/J.ACTAMAT.2023.118856.
[6] M.D. Hossain, T. Borman, C. Oses, M. Esters, C. Toher, L. Feng, A. Kumar, W. G. Fahrenholtz, S. Curtarolo, D. Brenner, J.M. LeBeau, J.P. Maria, Entropy landscaping of high-entropy carbides, Adv. Mater. 33 (2021), https://doi.org/10.1002/adma.202102904.
[7] T.J. Harrington, J. Gild, P. Sarker, C. Toher, C.M. Rost, O.F. Dippo, C. McElfresh, K. Kaufmann, E. Marin, L. Borowski, P.E. Hopkins, J. Luo, S. Curtarolo, D. W. Brenner, K.S. Vecchio, Phase stability and mechanical properties of novel high entropy transition metal carbides, Acta Mater. 166 (2019) 271–280, https://doi.org/10.1016/j.actamat.2018.12.054.
[8] L. Feng, W.G. Fahrenholtz, D.W. Brenner, High-entropy ultra-high-temperature borides and carbides: a new class of materials for extreme environments. https://doi.org/10.1146/annurev-matsci-080819, 2021.
[9] E. Chicardi, F.J. Gotor, M.D. Alcalá, J.M. Córdoba, Effects of additives on the synthesis of TiCxN1−x by a solid-gas mechanically induced self-sustaining reaction, Ceram. Int. 44 (2018) 7605–7610, https://doi.org/10.1016/j.ceramint.2018.01.179.
[10] J.M. Córdoba, E. Chicardi, F.J. Gotor, Development of multicomponent-multiphase materials based on (Ti,Ta,Nb)CxN1-x carbonitride solid solutions, Chem. Eng. J. 192 (2012), https://doi.org/10.1016/j.cej.2012.03.046.
[11] A.G. de la Obra, F.J. Gotor, E. Chicardi, Effect of the impact energy on the chemical homogeneity of a (Ti,Ta,Nb)(C,N) solid solution obtained via a mechanically induced self-sustaining reaction, J. Alloys Compd. 708 (2017), https://doi.org/10.1016/j.jallcom.2017.03.109.
[12] V. Suvorova, I. Khadyrova, A. Nepapushev, K. Kuskov, D. Suvorov, D. Moskovskikh, Fabrication and investigation of novel hafnium-zirconium carbonitride ultra-high temperature ceramics, Ceram. Int. 49 (2023) 23809–23816, https://doi.org/10.1016/j.ceramint.2023.04.222.
[13] A. Borrell, M.D. Salvador, V. García-Rocha, A. Fernández, E. Chicardi, F.J. Gotor, Spark plasma sintering of Ti yNb 1-yC xN 1-x monolithic ceramics obtained by mechanically induced self-sustaining reaction, Mater. Sci. Eng. 543 (2012), https://doi.org/10.1016/j.msea.2012.02.071.
[14] T. Che, H.R. Mao, R.F. Guo, P. Shen, Ultrafast synthesis and pressureless densification of multicomponent nitride and carbonitride ceramics, Ceram. Int. 49 (2023) 31530–31538, https://doi.org/10.1016/j.ceramint.2023.07.104.
[15] X. Jiang, P. Zhao, Y. Li, X. Wang, P. Jing, Y. Leng, Effect of carbon content on structure and properties of (CuNiTiNbCr)CxNy high-entropy alloy films, Ceram. Int. 50 (2024) 4073–4082, https://doi.org/10.1016/j.ceramint.2023.11.180.
[16] M. Yin, W. Liang, Q. Miao, H. Yu, W. Yao, K. Zang, Y. Sun, Y. Ma, Y. Wu, X. Gao, Y. Song, Microstructure, mechanical and tribological behavior of CrHfNbTaTiCxNy high-entropy carbonitride coatings prepared by double glow plasma alloy, Wear 523 (2023) 204751, https://doi.org/10.1016/J.WEAR.2023.204751.
[17] S. Ma, J. Ma, Z. Yang, Y. Gong, K. Li, G. Yu, Z. Xue, Synthesis of novel single-phase high-entropy metal carbonitride ceramic powders, Int. J. Refract. Metals Hard Mater. 94 (2021) 105390, https://doi.org/10.1016/J.IJRMHM.2020.105390.
[18] C. Jing, S.-J. Zhou, W. Zhang, Z.-Y. Ding, Z.-G. Liu, Y.-J. Wang, J.-H. Ouyang, Low temperature synthesis and densification of (Ti,V,Nb,Ta,Mo)(C,N) high-entropy carbonitride ceramics, J. Alloys Compd. 927 (2022) 167095, https://doi.org/10.1016/j.jallcom.2022.167095.
[19] R. Li, R.Y. Luo, N. Lin, A.Q. Li, X.C. Zhang, Y. Tang, Z.G. Wu, Z.Y. Wang, C. Ma, A novel strategy for fabricating (Ti,Ta,Nb,Zr,W)(C,N) high-entropy ceramic reinforced with in situ synthesized W2C particles, Ceram. Int. (2022), https://doi.org/10.1016/j.ceramint.2022.07.242.
[20] J. Ma, S. Ma, X. Wang, Z. Xue, B. Li, T. Wang, Y. Liu, Preparation and mechanical properties of (Ti0.2Zr0.2V0.2Nb0.2Ta0.2)(C0.6N0.4)-Co high-entropy cermets, Mater. Char. 192 (2022), https://doi.org/10.1016/j.matchar.2022.112213.
[21] W. Zhang, Z. Xue, Z. Zou, H. Saxén, The ideal and regular mechanisms of hematite reduction reactions, Cryst. Res. Technol. 57 (2022), https://doi.org/10.1002/crat.202100240.
[22] V.S. Buinevich, A.A. Nepapushev, D.O. Moskovskikh, G.V. Trusov, K.V. Kuskov, S. G. Vadchenko, A.S. Rogachev, A.S. Mukasyan, Fabrication of ultra-high-temperature nonstoichiometric hafnium carbonitride via combustion synthesis and spark plasma sintering, Ceram. Int. 46 (2020) 16068–16073, https://doi.org/10.1016/j.ceramint.2020.03.158.